CFD modelling of NO$_x$ formation in biomass grate furnaces with detailed chemistry

Robert Scharler[1,2,3], Emil Widmann[1], Ingwald Obernberger[1,2,3]

[1] *Institute for Resource Efficient and Sustainable Systems, Graz University of Technology;*
Inffeldgasse 21b, A - 8010 Graz, Austria; Tel.: +43 (0)316 481300 34; Fax: +43 (0)316 481300 4; E-mail: scharler@rns.tugraz.at

[2] *AUSTRIAN BIOENERGY CENTRE GmbH;*
Inffeldgasse 21b, A - 8010 Graz, Austria

[3] *BIOS BIOENERGIESYSTEME GmbH;*
Inffeldgasse 21b, A - 8010 Graz, Austria

[4] *Technical University of Eindhoven, Department of Mechanical Engineering, Section Process Technology,*
Den Dolech 2, P.O. Box 513, 5600 MB Eindhoven, the Netherlands

ABSTRACT: This paper presents the development and testing of a new CFD NO$_x$ postprocessor for biomass grate furnaces with detailed reaction kinetics. A self-developed empirical fixed bed model was extended in order to describe the release of the most important nitrogen species from biomass fuel beds (NO and NH$_3$ as well as HCN in small concentrations). The data obtained were used as boundary conditions for gas phase NO$_x$ modelling based on the results from the preceding CFD simulation of the turbulent reacting flow in the combustion chamber. The Eddy Dissipation Concept (EDC) was combined with detailed reaction kinetics for NO$_x$ postprocessing. The ISAT algorithm for the tabulation of reaction kinetics during runtime was used in order to reduce computation time by up to two orders of magnitude per iteration. Simulations were performed for a 440 kW$_{th}$ pilot-scale (fuel: fibreboard) and for a 7.2 MW$_{th}$ industrial-scale biomass grate furnace (fuel: waste wood). The calculation results showed good qualitative and quantitative agreement with measurements. The developed CFD NO$_x$ postprocessor was successfully tested. 3D simulations of biomass grate furnaces with detailed reaction kinetics were performed for the first time in an engineering application. Continued tests and comparisons with measurements are necessary, however, in order to improve and validate the model. In conclusion, it can be stated that the newly developed NO$_x$ postprocessor allows NO$_x$ reduction measures in biomass grate furnaces to be investigated in detail and, therefore, is a powerful tool for the optimisation of furnace design and process control.

INTRODUCTION

A technical and economic optimisation of biomass combustion plants is necessary in order to establish them in the heat and power generation market. In that context,

compliance with NO_x emission limits is an important issue, especially for biomass fuels with strongly varying nitrogen concentrations. Sophisticated plant design and efficient operation are essential to avoid or minimise cost-intensive secondary NO_x-reduction measures. Researchers at Graz University of Technology (TU Graz) have successfully applied CFD to optimise the design of biomass grate furnaces with respect to flue gas burnout as well as to flow and temperature distribution (in order to minimise ash deposit formation and material stress). However, the simulation of NO_x formation was limited by the necessity to include far more complex chemistry than for combustion simulation, resulting in computation times that are far too long for engineering applications.

This paper presents the development and application of a new CFD NO_x postprocessor for biomass grate furnaces, which covers the release of NO_x precursors from the fuel bed and the subsequent CFD simulation of NO_x formation with detailed chemistry. It allows for a significant reduction of calculation time and, therefore, enables a detailed treatment of both turbulent flow and NO_x formation chemistry in 3D simulations of biomass grate furnaces. This permits a numerical investigation of NO_x emission reduction by primary measures in order to save expensive secondary measures costs. First test simulations were performed for a 440 kW_{th} pilot-scale (fuel: fibreboard) as well as for a 7.2 MW_{th} industrial-scale biomass grate furnace (fuel: waste wood).

TESTING OF THE CFD NO_X POSTPROCESSOR - MODELLED FURNACES

Measurements taken at a pilot-scale biomass grate furnace (nominal thermal capacity: 440 kW_{th}, see Fig. 1) during selected test runs were first compared with simulation results of the CFD NO_x postprocessor.
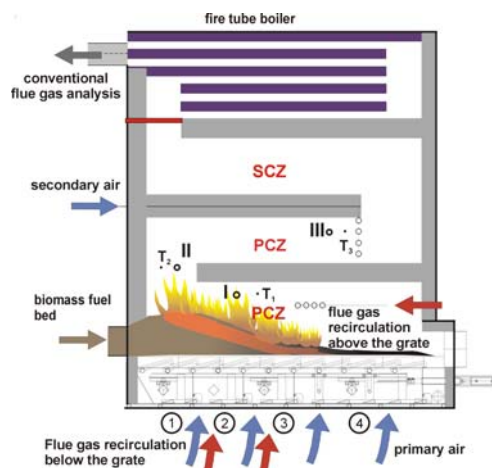

Fig. 1   Sketch of the pilot-scale biomass grate furnace
Explanations: PCZ...primary combustion zone; SCZ…secondary combustion zone; measurement positions FT-IR...I, II, III (large position rings); measurement positions thermocouples…T1, T2, T3 (small position rings); boundaries of CFD simulation: from entrance (fuel bed surface as well as re-circulated flue gas and secondary air inlet) to exit of the furnace (dark grey line)

Furthermore, the NO_x postprocessor was tested for a waste wood-fired 7.2 MW_{th} (nominal thermal capacity) industrial-scale biomass grate furnace (see Fig. 2). NO_x emissions measured after the fabric filter (conventional flue gas analysis) were compared with simulation results. Both furnaces are equipped with similar Low-NO_x technology.
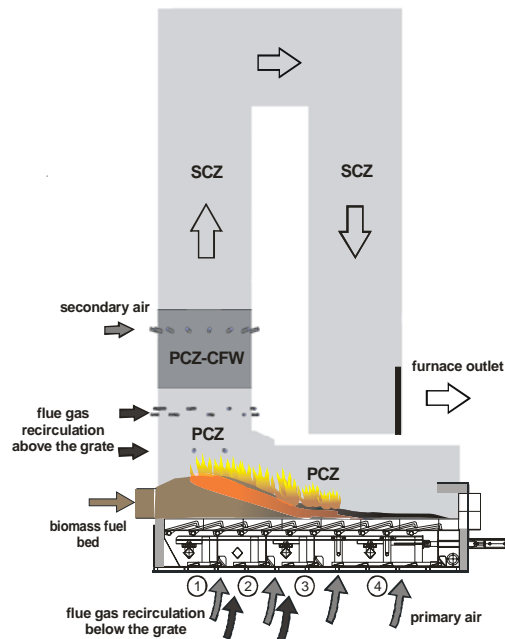

Fig. 2   Sketch of the industrial-scale biomass grate furnace
Explanations: PCZ...primary combustion zone; PCZ-CFW…primary combustion zone – section with cooled furnace walls; SCZ…secondary combustion zone; boundaries of CFD simulation: from entrance (fuel bed surface as well as re-circulated flue gas and secondary air inlet) to exit of the furnace (dark grey line)

EXPLANATION OF THE FURNACES INVESTIGATED

(1)   <u>Pilot-scale plant:</u> Low-NO_x grate furnaces are subdivided into a primary and a secondary combustion zone (see Fig. 1). The primary combustion zone is designed for sufficient flue gas residence time (about 0.6 – 0.8 seconds) and provides an oxygen lean atmosphere (air ratio $\lambda < 1$), in order to reduce nitrogen oxides (fuel NO_x) formed during the process of solid biomass combustion on the grate (fuel NO_x). The secondary combustion zone is designed as an oxygen rich zone (air ratio $\lambda > 1$) in order to ensure flue gas burnout. A further important feature of this furnace type is flue gas re-circulation for temperature control in the furnace. In order to make temperature control more efficient and, additionally, to improve turbulent mixing in the primary combustion zone, the combustion plant is equipped with staged flue gas recirculation, the flue gas being supplied above and below the grate. Improved turbulent mixing leads to faster CO burnout and more efficient NO_x reduction due to a break-up of flue gas strains arising from channelling in the fuel bed on the grate. This effect was confirmed by means of

experiments in the pilot-scale plant [10, 15]). Furthermore, these investigations showed that optimum NO_x reduction by primary measures can be achieved, when the mean residence time of the flue gas in the primary combustion zone exceeds 0.6 seconds at air lean conditions and bulk flow temperatures of about 950 to 1,150 °C [10, 15].

(2)   <u>Industrial-scale plant:</u> Since the waste wood-fired industrial-scale plant (see Fig. 2) is also designed as a Low-NO_x furnace, it is subdivided into a primary and secondary combustion zone. During regular full-load operation, the mean residence time of the flue gas in the primary combustion zone is about 0.7 seconds at air lean conditions and bulk flow temperatures of about 950 to 1,150 °C. The secondary combustion zone is designed as an air rich burnout zone ($\lambda > 1$) with the mean residence time of the flue gas exceeding 2.0 seconds (due to a legal regulation for waste wood combustion). According to the Low-NO_x concept considered, re-circulated flue gas is supplied below and above the grate in order to achieve efficient temperature control and turbulent mixing in the primary combustion zone (improved NO_x reduction and CO burnout). Since the industrial-scale furnace is fired with waste wood and therefore especially prone to ash slagging, additional measures have been provided. In the primary combustion zone, recirculated flue gas is injected at two positions above the grate in order to cool regions of excessive flue gas temperatures. Furthermore, the cylindrical part of the primary combustion zone, which is subjected to excessive temperatures, features cooled furnace walls.

DATA FROM TEST RUNS OF THE FURNACES INVESTIGATED

(1)   <u>Pilot-scale plant:</u> Concentrations of the flue gas species CH_4, CO, CO_2 and H_2O as well as the major NO_x precursor species NH_3 were measured by means of an in-house developed hot gas in-situ FT-IR absorption spectroscopy method [2] at three different locations of the combustion chamber (I, II, III – details see [10, 2]). The measurement values were averaged along the measurement path across the furnace cross-section. During one test run, measurements were taken at one FT-IR port only. Species concentrations of NO_x as well as O_2 and CO were measured at the boiler outlet with conventional flue gas analysis. In addition, temperature measurements were performed using thermocouples, which were positioned beside FT-IR ports I, II and III. Two test runs with fibreboard (Table 1) were selected due to the high nitrogen content of this fuel, resulting in the necessity of efficient NO_x reduction by primary measures. The effective air ratio in the primary combustion zone was varied from $\lambda < 1$ (see case A, Table 1) to $\lambda > 1$ (see case B, Table 1) in order to investigate the influence of air staging on NO_x reduction and to check the plausibility of simulation results. In this paper, only the measurement results concerning the N species will be discussed in detail (details about the basic combustion simulation can be found in [9 and 10]).

(2)   <u>Industrial-scale plant:</u> As already explained, the NO_x postprocessor was also tested in an industrial-scale application. Operating data of a waste wood-fired medium-scale biomass grate furnace derived from comprehensive monitoring test runs were taken as a basis for furnace simulation. The most relevant operating data are shown in Table 1. NO_x was measured after the fabric filter with conventional flue gas analysis (as was CO and O_2). Additionally, temperatures

were measured at several locations in the furnace using thermocouples. Only the comparison between calculated and measured NO_x emissions will be discussed in the paper.

Table 1 Important operating parameters of the furnaces investigated

operation data	pilot scale		industrial scale	
	case A	case B	monitoring test	
fuel	fibre board	fibre board	waste wood	
water content	10.60	10.60	17.70	wt% d.b.
nitrogen content	**3.06**	**3.06**	**1.20**	wt% d.b.
fuel power related to NCV	456	448	7,570	kW$_{th}$
recirculation ratio	0.49	0.46	0.18	-
lambda prim	**0.58**	**1.12**	**1.12**	**-**
lambda fuel bed eff	**0.78**	**1.50**	**1.12**	-
lambda primary eff	**0.97**	**1.63**	**1.29**	-
total air ratio	1.41	1.61	1.75	-
flue gas recirculation ratio	0.49	0.46	0.18	-
adiabatic flame temperature	933	888	1,120	°C
measured NO$_x$ emissions	**264**	**303**	**140**	ppmv

Explanations: flue gas recirculation ratio…mass of flue gas re-circulated / mass of total flue gas in the furnace; $\lambda_{fuel\ bed\ eff}$…(effective) air ratio in/above the fuel bed based on the total amount of primary air and re-circulated flue gas supplied below the grate; $\lambda_{primary\ eff}$…(effective) primary air ratio based on the total amount of primary air and the total amount of re-circulated flue gas; total air ratio…air ratio based on the total amount of injected air (primary + secondary air)

MODELLING

The simulation of solid biomass combustion on the grate and CFD simulation of turbulent reactive flow in the combustion chamber were performed via forward coupling. An in-house developed empirical model was used for the combustion of solid biomass on the grate. This model supplies velocities, species concentrations (CH_4, CO, CO_2, H_2, H_2O, O_2 as well as NH_3, HCN and NO) and temperatures of the flue gas above the surface of the fuel layer as boundary conditions for the subsequent CFD simulation of turbulent reacting flow in the furnace.

Under the assumption that the NO_x formation reactions do not significantly influence the flow pattern in the furnace, a time saving 2-step approach was applied for CFD simulations. Basic gas phase combustion simulation was done using the Realizable k-ε Turbulence Model, the Eddy Dissipation / Finite Rates Kinetics Combustion Model in combination with a global methane 3-step mechanism (CH_4, CO, CO_2, H_2, H_2O and O_2) and the Discrete Ordinates Radiation Model were used for basic gas phase combustion simulation in the case. The sub-models were validated for combustion simulation in biomass furnaces by lab-scale test cases [10]. The overall CFD model for biomass grate furnaces (basic combustion simulation) was validated with the measurements at the pilot-scale grate furnace (details see [9 and 10]).

The subsequent CFD simulation of gas phase fuel NO_x formation in a postprocessing mode was performed using the Eddy Dissipation Concept in

combination with a detailed reaction mechanism with 50 species and 253 reactions (Kilpinen 92, see [4]) which was developed for NO_x kinetics in biomass combustion systems. This model allows for a detailed consideration of both flow and chemistry.

EMPIRICAL FUEL BED COMBUSTION MODELLING – BASIC VERSION

An empirical model was applied for the combustion of the solid biomass fuel on the grate. The results (mass and energy fluxes from the fuel bed to the gas phase) were used as boundary conditions for subsequent CFD simulation. The model basically consists mainly of three parts (for a more detailed description see [10]).

(1) One-dimensional profiles along the grate, which describe the degradation of the fuel components C, H and O as well as fuel drying, were defined based on assumptions and experimental data (experiments at a lab-scale pot furnace reactor and test runs at a pilot-scale grate furnace, see [10]). Experiments have shown a linear correlation between the individual components H_2O, C, H and O released from the biomass fuel bed, which allowed for a simplification of the model (a profile must be defined only for one fuel component).

(2) Conversion parameters, which describe the formation of the most important flue gas components for combustion simulation (CH_4, CO, CO_2, H_2, H_2O and O_2) are defined based on assumptions as well as experimental [12] and literature data [5].

(3)   (1) and (2) permit a discrete balancing of mass and energy fluxes released from the fuel bed along the grate.

RELEASE OF NITROGEN SPECIES FROM THE FUEL BED ON THE GRATE – EXTENSION OF THE EMPIRICAL FIXED BED MODEL

Since NO_x formation in biomass grate furnaces usually originates almost exclusively from oxidation of fuel bound nitrogen (fuel NO_x), the release of NO_x precursors from the fuel bed is a crucial factor for a successful modelling of the overall furnace. However, the model of nitrogen release and conversion from the fuel is closely linked to the model applied for fix bed combustion. As already discussed above, a detailed treatment of the physical and chemical processes involved seems not applicable at the present stage. The release of nitrogen species from the fuel bed was modelled within the framework of the empirical model, following steps (1) to (3) of the previous chapter.

Fuel N is converted either to N_2 or to the NO_x precursors NH_3 and HCN as well as NO. Based on literature data [12] and lab-scale pot-furnace (batch reactor) experiments [12], the conversion parameters of fuel nitrogen depend on the local air ratio λ and the nitrogen content of the fuel. While HCN is the most important NO_x precursor in coal combustion, pot furnace experiments [12] with woody biomass fuels (fibreboard and waste wood in the present case) showed NH_3 to be the dominant NO_x precursor released from the fuel bed. Only negligible concentrations of HCN were detected in those experiments. In the course of earlier experiments performed on an understoker furnace by Keller [5], HCN and NH_3 were found in concentrations of the same order of magnitude. Consequently two different sets of model parameters were derived. The first set is based on the nitrogen conversion rates obtained from the pot furnace experiments (chiefly NH_3), the second is based on the conversion rates found at the understoker furnace (NH_3 and HCN).

CFD MODELLING OF TURBULENT REACTING FLOW

The CFD combustion simulation, which provides the basis for NO_x postprocessing, was performed with the unstructured CFD solver FLUENT 6 (see [13]). The turbulent reacting flow was modelled using the Realizable k-ε Model (turbulence), the Discrete Ordinates Model (radiation) as well as the Eddy Dissipation Model of Magnussen and Hjertager [7] (turbulent gas phase combustion) in combination with a global methane 3-step reaction mechanism of Brink [1] including the species CH_4, CO, CO_2, H_2, H_2O and O_2.

The EDM, in combination with reaction kinetics, serves to calculate the reaction rate as the lowest (limiting) value of mixing rates proportional to the break-up of fuel, oxygen and product eddies as well as a kinetic rate without taking the influence of turbulent fluctuations into account. The EDM is reasonably accurate for most industrial applications, numerically robust and applicable to premixed, non-premixed and partially premixed combustion but cannot account for strong coupling between turbulence and reaction kinetics. If reaction kinetic effects become important – NO_x formation in this application – the EDM combined with global kinetics is not suitable. Another disadvantage is the fact that the empirical model parameter (A_{mag}), which determines the mixing rate calculated with the EDM, is not universally valid. Calculations of a lab-scale test case [10] as well as the already mentioned comparison with the measurements at the lab-scale biomass grate furnace have shown that the originally proposed value of $A_{mag} = 4.0$ (Magnussen and Hjertager [7]) is too high for this application (for details see [9, 10]). A value of $A_{mag} = 0.6$ was found to be suitable for the simulation of biomass grate furnaces.

The constant increase in computing power allows for the application of more advanced CFD models for industrial applications. Various combustion models are thus currently being tested for 3D furnace simulations in order to overcome the above mentioned weaknesses of the EDM, which is important for a more detailed investigation of various combustion phenomena.

CFD NO$_X$ POSTPROCESSING

The Eddy Dissipation Concept [3, 6] is an advancement of the Eddy Dissipation Model of Magnussen and Hjertager [7] and allows to account for the interaction of turbulence and multi-step chemistry. Both models belong to the group of eddy break-up models, which are momentum methods. The implementation in FLUENT is based on the paper of Gran and Magnussen [3]. The reaction rate is an empirical expression based on the assumption that the reactions occur mainly in the smallest length scales of the turbulent energy cascade, called "fine structures", where turbulent energy is dissipated and which are on the order of the Kolmogorov length scale in 1 or 2 dimensions. The mass fraction of the fine structure regions is calculated as

$$\gamma = \left(\frac{3C_{D2}}{4C_{D1}^2} \right)^{1/4} \left(\frac{\nu^* \tilde{\varepsilon}}{\tilde{k}^2} \right)^{1/4} , \qquad \text{equation 1}$$

with the model constants $C_{D1} = 0.134$ and $C_{D2} = 0.5$, the Favre-averaged ($\tilde{}$) values k [m²/s²] and ε [m²/s³] of the mean flow and the kinematic viscosity ν* [m²/s] in the fine structures. The mass fraction γ^* [-] of the fine scales in the flow is modelled as

$$\gamma^* = \gamma^3 .$$
<div align="right">equation 2</div>

The time scale τ* [s] for the mass transfer between the fine structures and the surroundings or the reaction time in the fine scales is modelled as

$$\tau^* = \left(\frac{C_{D2}}{3}\right)^{1/2} \left(\frac{\nu^*}{\tilde{\varepsilon}}\right)^{1/2} .$$
<div align="right">equation 3</div>

Then, the net production rate R_n [kg/m³s] of species i can be expressed as

$$R_i = \frac{\overline{\rho} \cdot \gamma^2 \chi}{\tau^*} \left(Y_i^* - Y_i^0\right).$$
<div align="right">equation 4</div>

with the time-averaged value of the density ρ [kg/m³], the reacting fraction χ [-] ($0 \leqq \chi \leqq 1$) of the fine structures and the mass fraction Y [-] in the fine structures (*) and the surroundings (^{0}) of the fine structures. The mass fraction of the Favre-averaged mean flow ($\tilde{}$) can be expressed from the quantities in the fine structures and the surroundings as follows:

$$\tilde{Y} = \gamma^3 \chi Y^* + (1 - \gamma^3 \chi) Y^0 .$$
<div align="right">equation 5</div>

For finite rate kinetics, the reacting fraction χ of the fine structures can be set to 1. Substituting equation 5 in equation 6, the net production rate R_i of species i is:

$$R_i = \frac{\overline{\rho} \cdot \gamma^2}{\tau^* \left(1 - \gamma^3\right)} \left(Y_i^* - \tilde{Y}_i\right).$$
<div align="right">equation 6</div>

In equation 6 the concentrations in the fine structures are unknown. If the fine structures are considered as ideal reactors, the concentrations (and temperatures) in the fine structures, which may differ considerably from the locally averaged values, can be calculated and the equation system is closed.

The EDC was used in various versions (e.g. [1, 3]). The EDC, however, was not implemented in commercial CFD codes until quite recently. The major reason is that fine structures are originally treated as perfectly stirred reactors (PSR) [6]. This circumstance may lead to convergence problems during the iterative solution of the highly non-linear algebraic equation system and causes a considerable numerical effort. It was shown [14] that a plug flow reactor (PFR) model can be implemented in the EDC instead of a PSR, which leads to a considerable simplification of the numerical solution process. An integration of the reaction rates over the residence time (or reaction time) in the fine structures via a time-stepping method can then be used for the calculation of the fine structure values.

Based on this assumption, the EDC was implemented in the CFD code FLUENT. In combination with the ISAT (In-Situ Adaptive Tabulation) algorithm by Pope [11], an enormous reduction of calculation time is possible. This method involves a tabulation of the chemical state space (species concentrations, temperature, pressure) during the CFD simulation, resulting in speed-up factors of up to 100 per iteration. The interpolation error tolerance thus strongly determines the accuracy of the simulation results and the time needed for the generation of the ISAT table, which can be in the order of days.

A coupled simulation of flow and chemistry, however, is too time-consuming at the present development stage of the NO_x formation model. The 2-step approach as mentioned was thus chosen and the NO_x formation is simulated in a postprocessing mode.

INTEGRATION OF REACTION KINETICS

The detailed kinetic scheme used in the model should give a comprehensive description of all relevant NO_x formation processes, and most important, fuel NO_x formation. Additionally, the mechanism should meet the technical restriction of the ISAT algorithm used, i.e. a maximum of 50 species.

The Kilpinen 92 mechanism with 50 species and 253 reactions, which describes nitrogen oxide chemistry during C1 and C2 hydrocarbon oxidation, met these requirements [4]. Ideal reactor calculations were performed (PFR and PSR) to compare this mechanism against the results of the more comprehensive reaction mechanisms Glarborg 98 and Kilpinen 97, which are widely used for biomass combustion systems. In the expected range of application (initial gas phase concentrations, atmospheric pressure and temperatures in the fine structures up to 1,400 °C and 2,000 °C in small regions above the fuel bed for some exceptions) no major deviations were found [12].

DISCUSSION OF RESULTS

As already mentioned, measurements were compared with simulation results for a pilot-scale (440 kW$_{th}$) and an industrial-scale (7.2 MW$_{th}$) biomass grate furnace. Additionally, a qualitative comparison of the CFD simulation results with literature data and lab-scale pot furnace experiments was performed for both furnaces.

SIMULATION OF THE PILOT-SCALE PLANT

Simulations were performed for two selected test runs with an effective air ratio $\lambda<1$ (case A) and $\lambda>1$ (case B) in the primary combustion zone. A comprehensive discussion and validation of the results concerning the basic CFD combustion simulation can be found in [9 and 10]. Temperature and O_2 profiles are shown in Fig. 3. The maximum flue gas temperatures were obtained for the primary combustion zone, at about 1,200 °C for case A ($\lambda < 1$) and 1,050 °C for case B ($\lambda > 1$). The corresponding fine scale temperatures increased by about 150 °C in some smaller regions of the primary combustion zone, but did not considerably exceed the above mentioned maximum flue gas temperatures. Therefore, no figures of the calculated fine scale temperatures are shown here.
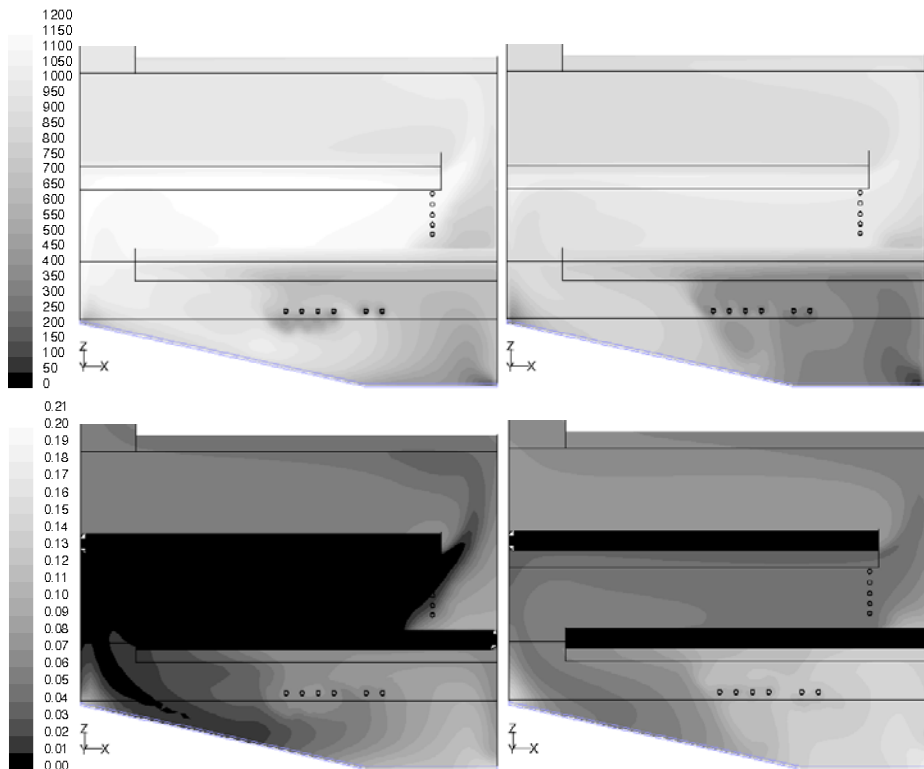
Fig. 3: Simulated profiles of flue gas temperature [°C] (top) and mole fraction of O_2 [-] (bottom) for the pilot-scale plant (figures left…case A; figures right…case B)

The simulated NO_x emissions at the furnace outlet in all cases consisted of NO in major concentrations and NO_2 only in minor concentrations (< 10 ppmv), which is in agreement with experience (measurements at the outlet of various biomass grate furnaces with conventional flue gas analysis) and measurements at a lab-scale pot-furnace reactor [12].

For case A, a sensitivity analysis concerning the influence of the release of fuel NO_x precursors was performed. Agreement between the measured NO_x emissions at boiler outlet (264 ppmv) and the corresponding simulation was good for both species release profiles (see Table 2).The error for the case with a major release of NH_3 and only minor concentrations of HCN (based on experimental investigations [12]; see Fig. 4, bottom) was smaller (about +10%) than for the case with a release of NH_3 and HCN (according to Keller [5]; see Fig. 4, top) (about +25%).

Based on these findings, case B was simulated with N-species release profiles from experiments (release of NH_3 in major concentrations). The results for case B were only about 10 % higher (see Table 2) than NO_x measurements at the boiler outlet (303 ppmv) and were thus in very good agreement.

Table 2   Comparison of measured and calculated NO_x emissions for the pilot-scale plant

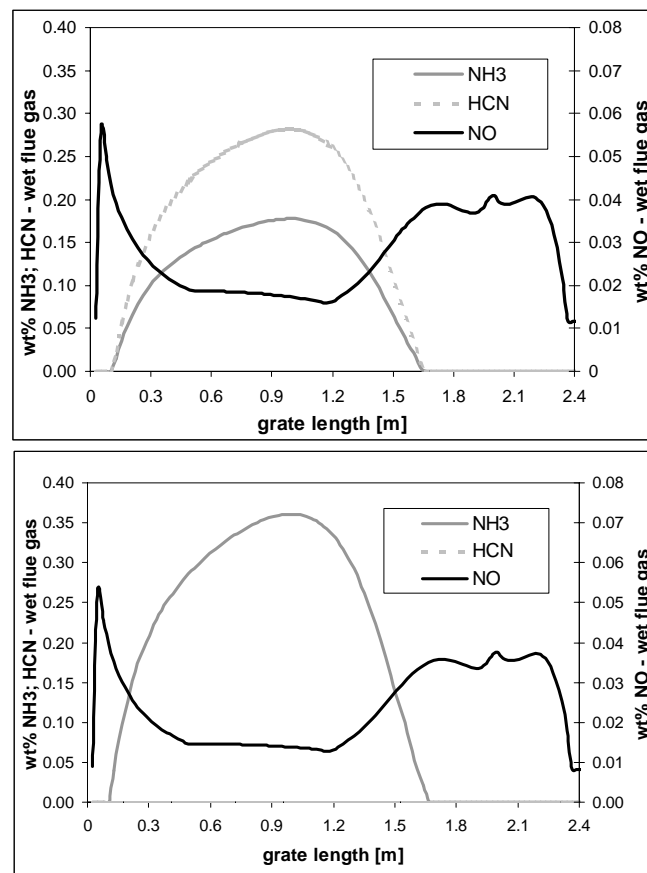|	source data empirical fixed bed model	NOx emissions [ppmv]	
		case A	case B
measured		264	303
calculated	Keller	335	-
	TU Graz	287	332

Fig. 4:   Calculated release profiles for the species NO, NH_3 and HCN [wt% wet flue gas] along the grate for case A
Explanations: top…based on Keller [5], NH_3 and HCN concentrations in same order of magnitude; bottom…based on experiments [12], NH_3 as dominating species

A comparison of case A and case B shows that for a smaller λ, or oxygen lean conditions, in the primary combustion zone (λ < 1), the simulated and measured NO_x

emissions are lower than for a higher λ, or oxygen rich conditions, in the primary combustion zone (> 1). This means that the trend of fuel NO_x reduction by air staging as an efficient primary measure could be reproduced with the CFD NO_x postprocessor.

Furthermore, the concentration levels of NH_3 and HCN at the furnace outlet were in agreement with experiments performed at a pot-furnace lab-scale reactor [12] as well as literature and experience with extractive FT-IR measurements at the outlet of various biomass grate furnaces. Measurements were carried out at FT-IR port III for case A and at FT-IR port II for case B. NH_3 concentrations were below the detection limit in both cases. Furthermore, FT-IR measurements at the lab-scale pot furnace reactor showed that NH_3 is not immediately consumed above the fuel bed and is still present at a height of about 20-40 cm above the surface of the fuel bed. The simulations predicted that NH_3 is not immediately consumed above the fuel bed but nearly completely in the primary combustion zone, depending on the effective air ratio in the primary combustion zone (earlier for larger λ). This is in qualitative agreement with measurements at the pilot-scale plant and the pot-furnace reactor.
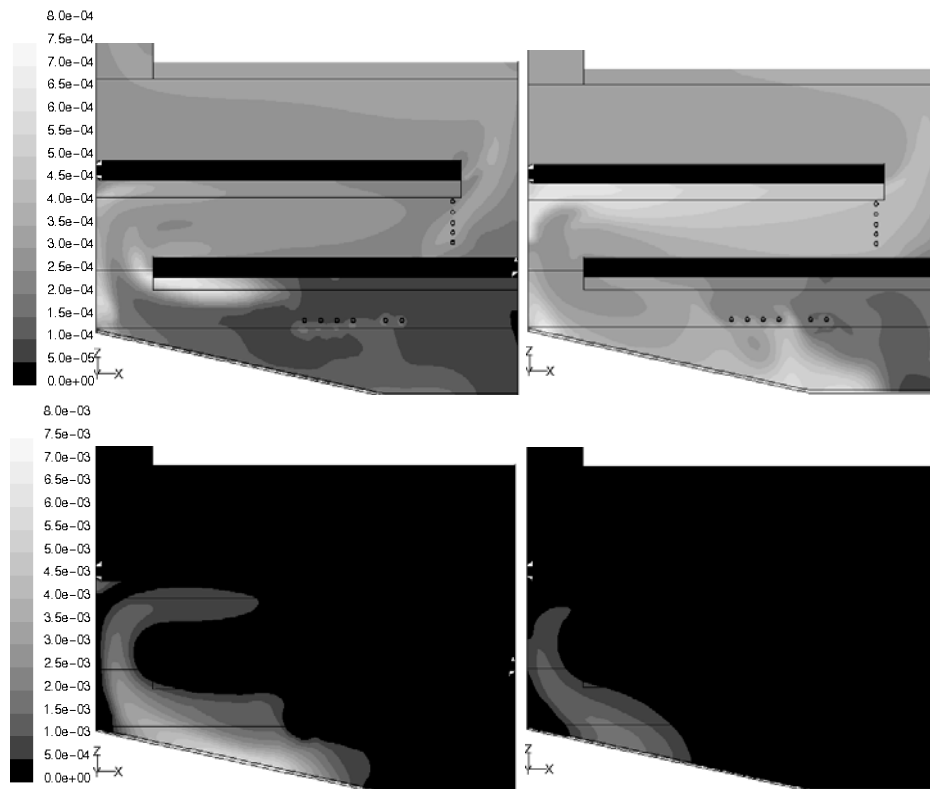

Fig. 5:   Simulated profiles of mole fractions of NO_x [-] (top) and NH_3 [-] (bottom) for the pilot-scale plant (figures left…case A; figures right…case B; release of NH_3 as dominant NO_x precursor species)

In conclusion, it can be stated that first simulation results are in sufficient qualitative and quantitative agreement with measurements at the pilot-scale plant (NO_x

measurements at boiler outlet and in-situ measurements of NH_3), species measurements at a lab-scale pot-furnace reactor as well as experience and literature data.

Furthermore, the results of the newly developed CFD based NO_x formation model were compared with results of previous NO_x postprocessors based on the Eddy Dissipation Model as well as a presumed PDF (Probability Density Function) Model and global reaction kinetics (for details see [12]). It was obvious, that all NO_x postprocessors based on global reaction kinetics failed to predict the NO_x formation process in biomass grate furnaces and therefore were outperformed by the newly developed NO_x postprocessor based on the EDC and detailed chemistry.

Moreover, the newly developed NO_x postprocessor allows simulation of other interesting and important species like NO_2, N_2O or radicals. As a consequence, the NO_x postprocessor based on comprehensive chemistry gives a deeper insight in the NO_x formation process within the furnace than the formerly tested versions based on global chemistry. This can also be identified by means of the spatially inhomogeneous NO profiles in the primary combustion zone (see Fig. 5), which indicate kinetic or mixing effects. This turns the newly developed NO_x formation model into a powerful tool for the investigation of NO_x formation in biomass grate furnaces.

SIMULATION OF THE INDUSTRIAL-SCALE PLANT

Simulations with operating data of a selected test run during a comprehensive monitoring period were performed for the industrial-scale furnace. According to the basic combustion simulation (see Fig. 6), the furnace is not in the optimum Low-NO_x operation mode concerning flue gas temperatures in the primary combustion zone at up to 1,400 °C (target area of bulk flow 950°C – 1,150 °C; see [15]) and effective air ratios in the primary combustion zone ($\lambda > 1$; should be < 1; see also [10] and [15]). Nevertheless, the NOx emissions measured after the fabric filter were relatively low (140 ppmv). This indicates that a good and effective mixing of the unburned flue gas with re-circulated flue gas is important for effective NO_x reduction, which is the case for this furnace (simulations show temperature peaks due to increased reaction rates in the near-field of the flue gas recirculation nozzles above the fuel bed – see Fig. 6). Furthermore, the simulated temperatures above the fuel bed are probably too high, which will be discussed later.
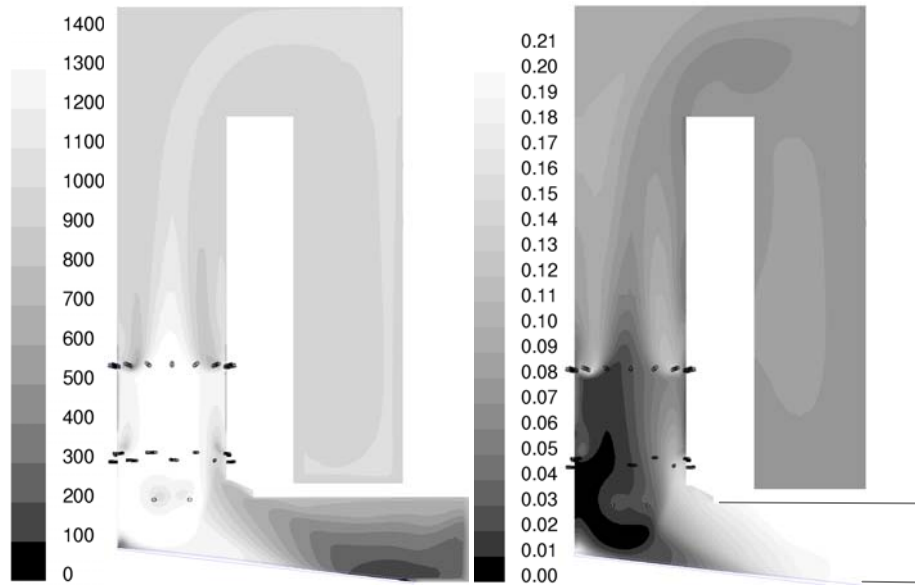
Fig. 6:   Simulated profiles of flue gas temperatures [°C] (left hand figure) and mole fractions of O_2 [-] (right hand figure)

Based on this basic combustion simulation, two NO_x postprocessing simulations were performed with release profiles based on experiments (NH_3 in major concentrations, HCN in minor concentrations) and literature data from Keller (NH_3 and HCN in major concentrations). Both simulations predicted the same trends for the species NH_3, HCN, NO and NO_2 as the simulations for the pilot-scale plant. Again, NO_x emissions based on the profiles with a major release of NH_3 are closer to the measurements (see Table 3). This is a further confirmation that NH_3 is the main precursor species of gas phase NO_x formation in wood combustion systems. The NO_x emissions were calculated with reasonable accuracy. The simulated emissions were about 230 ppmv, which is a larger deviation (+65 %) from the measurements than for the simulations performed for the pilot-scale plant (see Table 3).

Table 3 Comparison of measured and calculated NO_x emissions for the industrial-scale plant

	source data empirical fixed bed model	note	NOx emissions [ppmv]
measured			140
calculated	Keller		293
	TU Graz		233
	TU Graz	lowered temperature peaks	213

In this case, the major reason might be the simulated flue gas temperatures in the primary combustion zone, especially above the fuel bed, which are probably too high (unfortunately no reliable temperature measurements in this region were available during the test runs). On the one hand, predicted temperatures above the fuel bed tend to be too high due to the negligence of radicals in basic combustion simulation with the EDM. More sophisticated combustion models (like the EDC) are thus currently being tested. Furthermore, flue gas strains arising from the fuel bed, which were visually observed at the industrial-scale plant, cause a slowdown of the chemical reactions but were not modelled. Therefore, appropriate models for strain formation will be developed. Moreover, the temperatures in the fine structures determining the reaction rate are higher than the average temperatures in the main combustion zone. In the case investigated here the fine scale temperatures in a small region above the fuel bed were about 2,000 °C (see Fig. 7), which leads to the formation of thermal and prompt NO_x in the fine structures. In this region the simulated NO_x concentration (see Fig. 7) is highest.

In order to investigate the influence of flue gas temperatures on local NO production, the locally averaged flue gas temperatures from basic combustion simulation were lowered to a maximum value of about 1,150 °C with a damping function. Nevertheless, the corresponding values in the fine structures, which were calculated during NO_x postprocessing, still increased to about 1,800 °C. As a consequence, the calculated NO_x emissions dropped, but were still about 50% above the measured values (see Table 3).
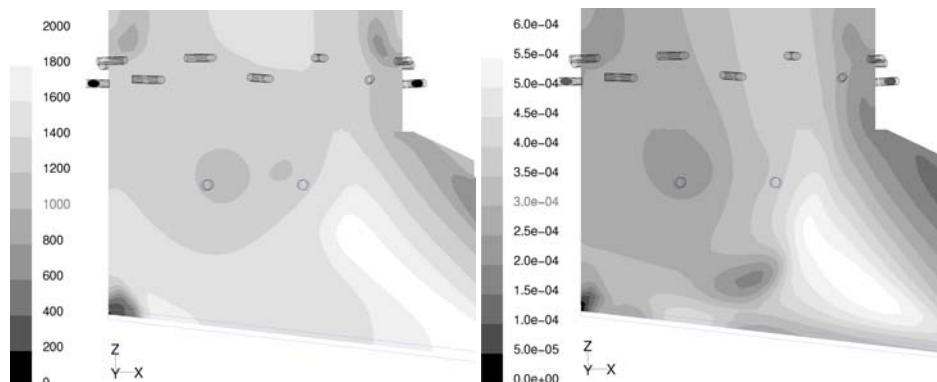

Fig. 7:   Simulated profiles of fine scale temperature [°C] (left hand figure) and mole fraction of NO [-] (right hand figure) in the primary combustion zone of the industrial-scale furnace

From these results it becomes obvious that the empirical fixed bed model, which is reasonably accurate for CFD combustion simulation, can also lead to errors in the prediction of NO_x formation. The results of the NO_x postprocessor (EDC in combination with detailed reaction kinetics) depend to a certain amount on the boundary conditions (profiles of flue gas velocity, temperature, species concentrations and turbulence), which are calculated with the empirical fixed bed model. More tests of the NO_x postprocessor are necessary in order to investigate this sensitivity. Based on these results, the empirical fixed bed model will be improved or replaced by a more

fundamental model with transport equations (if the side constraint of reasonable computation times for engineering applications is fulfilled).

TIME NEEDED FOR THE SOLUTION PROCEDURE

First test runs for the pilot-scale plant (size of the CFD grid: 275,000 cells) with the newly developed NO_x postprocessor based on detailed chemistry took about 2 weeks on a PC (2.4 GHz). By optimising the solution procedure, the time was further reduced to about 1.5 weeks. A parallelised calculation (PC cluster with 4 nodes) took about 1 week. A further considerable reduction will soon be possible due to an improvement of the ISAT tabulation algorithm, which has been a major time-consuming factor. This improvement will make it possible to save, load and adapt the ISAT table during parallel calculation.

First test runs for the industrial-scale plant (size of the CFD grid: 420,000 cells) needed considerably longer than the calculations for the pilot-scale plant. Parallel calculation on a PC cluster with 6 machines took about 2-3 weeks due to the higher number of tabulated values (same interpolation error tolerance). As a consequence, the time needed for the calculation is hard to estimate due to the fact that the time needed to fill the ISAT table depends on the manifolds of the chemical reaction system. A considerable reduction is expected, however, from the new version of the ISAT table.

Nevertheless, a reduced NO_x reaction mechanism is currently being developed in order to allow for a reduction of calculation time and to make this time-consuming method more attractive for industrial applications, even with very large geometries. Furthermore, a coupled simulation of both combustion and NO_x formation reactions with the EDC and this reduced mechanism is planned in order to overcome weaknesses of the basic combustion simulation with the EDM and global combustion chemistry.

SUMMARY AND CONCLUSIONS

A new CFD NO_x postprocessor for biomass grate furnaces was developed taking into consideration detailed reaction kinetics. It is based on an empirical fixed bed combustion model, which was extended to the release of nitrogen containing species (NH_3, HCN and NO) as well as the EDC in combination with the Kilpinen 92 mechanism (with 50 species and 253 reactions) and the ISAT algorithm for the tabulation of chemical reactions.

The CFD NO_x postprocessor was successfully tested for 3D simulations of biomass grate furnaces, which were performed for the first time with detailed chemistry. Simulations were performed for a 440 kW_{th} pilot-scale (two test runs) as well as a 7.2 MW_{th} industrial-scale biomass grate furnace (selected test run during a monitoring period), both equipped with Low-NO_x technology. The simulations required about 1 to 3 weeks of computation time, but a significant reduction is possible by parallel processing and a recently improved ISAT algorithm. For both furnaces, all relevant nitrogen species concentrations (NO_x precursors NH_3 and HCN as well as NO and NO_2) showed good qualitative agreement with measurements under different operating conditions as well as data from lab-scale experiments and literature.

Results from pot-furnace experiments with woody biomass fuels showed that NH_3 is the most dominant precursor species for fuel NO_x formation in biomass grate furnaces. This was verified by a comparison of NO_x emissions measured at the furnace

outlet with simulation results of the NO_x postprocessor. For both furnaces, the NO_x postprocessor simulations with release profiles based on experiments (NH_3 in major concentrations, HCN in minor concentrations) were closer to NO_x measurements than the simulation results with profiles based on literature data from Keller (NH_3 and HCN in concentrations of the same order of magnitude). For the pilot-scale plant, the agreement of predicted NO_x emissions with NO_x measurements at boiler outlet was very good for the test runs with air lean conditions ($\lambda < 1$) and air rich conditions ($\lambda > 1$) in the primary combustion zone. The deviation between measurements and simulation was about +10 % for both operating conditions. The effect of air staging was thus reproduced correctly.

For the industrial-scale plant, the agreement of predicted NO_x emissions with measurements at boiler outlet was reasonable, but the deviation between measurements and simulations was larger (+50% to +65 %). The weaknesses of the basic combustion simulation (with the EDM) and the empirical fixed bed combustion model seem to be the major reasons for the larger deviations in this case.

The empirical fixed bed model is thus being improved based on experiments performed at a lab-scale pot furnace as well as test runs at a pilot-scale biomass grate furnace. Additionally, a fixed bed combustion model based on transport equations is being tested for biomass grate furnaces (concerning suitability for engineering applications). Moreover, the formation of strains due to channelling in the fuel bed will be modelled. Furthermore, various advanced gas phase combustion models are now being tested for the modelling of biomass furnaces. A reduced NO_x reaction mechanism is currently being developed in order to further reduce calculation time and to make this time-consuming method more attractive for industrial applications, even with very large geometries. Additionally, the application of a reduced NO_x reaction mechanism will make a coupled simulation of both combustion and NO_x formation reactions possible, which allows to overcome the weaknesses of basic combustion simulation with the EDM and global combustion chemistry.

In conclusion, it can be stated that the newly developed NO_x postprocessor allows NO_x reduction measures in biomass grate furnaces to be investigated in detail and, therefore, represents a powerful tool for the optimisation of furnace design and process control. Continued tests and comparisons with measurements are necessary in order to improve and validate the model (including the fixed bed and the gas phase combustion sub-models).

LITERATURE

1   Brink, Anders, 1998: Eddy Break-Up based models for industrial diffusion flames with complex gas phase chemistry. Ph.D. thesis, Abo Akademi University, Finland, ISBN 952-12-0302-1

2   Fleckl, Thomas, 2001: Verbrennungsdiagnostik an Biomasserostfeuerungen mittels FT-IR in-situ Absorptionsspektroskopie, Ph.D. thesis, Graz University of Technology, Austria.

3   Gran, I., Magnussen, B., 1996: A numerical study of a bluff-body stabilized diffusion flame. Part 2. Influence of combustion chemistry. In: Combust. Sci. and Tech., Gordon and Breach Science Publishers (Ed.), Vol. 119, pp. 191-217

4   Kilpinen, P., 1992: Kinetic Modeling of Gas-Phase Nitrogen Reactions in Advanced Combustion Processes, Ph.D thesis, Abo Akademi University, Department of Chemical Engineering, Finland, Report 92-7, ISBN 951-650-132-X.

5   Keller, R., 1994: Primärmaßnahmen zur NOx-Minderung bei der Holzverbrennung mit dem Schwerpunkt Luftstufung, Research Report No. 18 (1994) Laboratorium für Energiesysteme (Ed.), ETH Zürich, Switzerland.

6   Magnussen, B. F., 1989: Modeling of pollutant formation in gas turbine combustors based on the Eddy Dissipation Concept. Presented at the CIMAC – Conference, June 4-9, 1989, Tianjin, China.

7   Magnussen, B. F., Hjertager, B. H., 1976: On mathematical modeling of turbulent combustion with special emphasis on soot formation and combustion. In: Proceedings of the 16th Symp. (Int.) on Combustion, pp. 719-729, The Combustion Institute (Ed.), Pittsburgh, USA

8   Scharler R., Obernberger I., 2000: Numerical optimisation of biomass grate furnaces. In: Proceedings of the 5th European Conference on Industrial Furnaces and Boilers, April 2000, Porto, Portugal, INFUB (Ed.), Rio Tinto, Portugal, ISBN-972-8034-04-0

9   Scharler R., Fleckl, T., Obernberger, I, 2003: Modification of a Magnussen Constant of the Eddy Dissipation Model for biomass grate furnaces by means of hot gas in-situ FT-IR absorption spectroscopy, Progress in Computational Fluid dynamics, Vol. 3, Nos.2-4, pp. 102-111

10 Scharler, R., 2001: Entwicklung und Optimierung von Biomasse-Rostfeuerungen durch CFD-Analyse, Ph.D. thesis, Graz University of Technology, Austria.

11 S. B. Pope, 1997: Computationally efficient implementation of combustion chemistry using in-situ adaptive tabulation, Combustion Theory and Modeling, Volume 1, pp. 41-63.

12 Obernberger, I., Widmann, E., Scharler, R., 2003: Entwicklung eines Abbrandmodells und eines NO_x-Postprozessors zur Verbesserung der CFD-Simulation von Biomasse-Festbettfeuerungen. Reports from energy and environment research, report No. 31/2003, Ministry for Transport, Innovation and Technology (Ed.), Vienna, Austria.

13 FLUENT 6.1 User's Guide, Volume 2, Fluent Inc., February 2003.

14 Jessee. J. P., Gansman, R.F., Fiveland, W.A., 1993: Calculation of chemical reacting flows using finite rate kinetics, HTD-Vol. 250, pp. 43-53, Heat Transfer in Fire and Combustion System, ASME (ed.)

15 Weissinger A., 2002: Experimentelle Untersuchungen und theoretische Simulationen zur NO_x-Reduktion durch Primärmaßnahmen bei Rostfeuerungen, Ph.D. thesis, Graz University of Technology, Austria.